

Key Points:

- A chemical difference between crystalline and amorphous phase was observed in partially amorphized plagioclase from meteorite DEW 12007
- Partial melting could induce the more albite (or anorthite)-rich amorphous plagioclase in partially amorphized plagioclase grain
- The formation mechanism of amorphous plagioclase in meteorites can be revealed by both morphological and chemical analyses

Supporting Information:

- Supporting Information S1

Correspondence to:

H. N. Kim,
hnkim@kongju.ac.kr

Citation:

Kim, H. N., Park, C., Park, S. Y., Kim, H., & Kim, M. S. (2019). Partial melting-induced chemical evolution in shocked crystalline and amorphous plagioclase from the lunar meteorite Mount DeWitt 12007. *Journal of Geophysical Research: Planets*, 124, 1852–1863. <https://doi.org/10.1029/2019JE005998>

Received 7 APR 2019

Accepted 19 JUN 2019

Accepted article online 26 JUN 2019

Published online 12 JUL 2019

Partial Melting-Induced Chemical Evolution in Shocked Crystalline and Amorphous Plagioclase From the Lunar Meteorite Mount DeWitt 12007

Hyun Na Kim¹ , Changkun Park² , Sun Young Park², Hwayoung Kim², and Min Sik Kim¹

¹Department of Earth and Environmental Sciences, Kongju National University, Gongju, South Korea, ²Division of Polar Earth-System Sciences, Korea Polar Research Institute, Incheon, South Korea

Abstract Determining the formation mechanism of maskelynite is essential to understanding the shocked environments of meteorites on their parent bodies. Maskelynite has been accepted as a diaplectic glass for several decades, but there have been suggestions that it is a normal glass quenched from a dense melt. Morphological characteristics have been generally investigated to identify the formation mechanism of amorphous plagioclase in meteorites, but the chemical difference between crystalline and amorphous plagioclase has not been fully understood. In this study, we investigated the morphological, atomic-scale structural, and chemical characteristics of amorphous plagioclase in the lunar meteorite DEW 12007 to constrain its formation mechanism via chemical analysis. The morphological characteristics showed that plagioclase was partially converted into amorphous phase through partial melting. Two-dimensional Raman mapping confirmed the structural difference between amorphous and crystalline regions. Quantitative chemical analyses revealed that the amorphous regions were more albite-rich than the crystalline regions, likely due to the partial melting of plagioclase. Under shocked conditions, the partial melting of plagioclase induced a chemical variation between amorphous and crystalline regions. The morphological and structural changes correspond well with the chemical variations, indicating that amorphization induced such variations. The chemical differences between amorphous and crystalline plagioclase in other meteorites also could be understood to be the results of partial melting. Thus, the chemical differences between amorphous and crystalline plagioclase in partially amorphized grains could elucidate the formation mechanism of amorphous plagioclase in many meteorites.

Plain Language Summary Amorphous plagioclase is a type of mineral used as a shock indicator in meteorites. It can be formed by solid state transformation or melting depending on the shock environment. We studied the morphology and chemical characteristics of plagioclase grains from the lunar meteorite DEW 12007, found in Antarctica. A portion of each plagioclase grain was changed into an amorphous phase during the shock event while the rest was left as a crystalline phase. The morphology of the plagioclase grain indicates that the partial amorphization occurred by partial melting, not by solid state transformation. Partial melting also caused a chemical difference between the amorphous and crystalline parts of the plagioclase grain. Previous works showed that the solid state transformation does not generate a chemical difference between amorphous and crystalline parts of plagioclase grains. Thus, the formation mechanism of amorphous plagioclase can be determined by comparing the chemical composition of amorphous and crystalline plagioclase in meteorites.

1. Introduction

Maskelynite, a diaplectic plagioclase glass usually found in meteorites, has long been recognized as an important indicator of shocked environments because it is formed by shock metamorphism under high pressure (Stöffler & Hornemann, 1972; Tschermak, 1872). Given this importance, many attempts have been made to determine the pressure and temperature conditions necessary for the formation of maskelynite (Fritz et al., 2005; Heymann & Hörz, 1990; Jaret et al., 2015; Kubo et al., 2010; Sims et al., 2019; Tomioka et al., 2010). These previous studies have mainly constrained the pressure and temperature history of maskelynite under the assumption that maskelynite is a diaplectic glass (Kubo et al., 2010; Tomioka et al., 2010). However, Chen and El Goresy suggested that maskelynite is a normal glass quenched from a dense melt (Chen & El Goresy, 2000; El Goresy et al., 2013). Since then, the formation mechanism of maskelynite has remained controversial and is not yet fully understood. If amorphous plagioclase can be formed by two

different mechanisms, it is necessary to designate them with two different names. In this study, we designated diaplectic glass-type amorphous plagioclase as “maskelynite” and normal glass-type amorphous plagioclase as “melt-quenched amorphous plagioclase,” according to the definition of maskelynite (Stöffler & Hornemann, 1972; Tschermak, 1872). Strictly speaking, the nomenclature “amorphous plagioclase” is also incorrect and “amorphous materials with the composition of plagioclase” should be used instead. However, the shorter amorphous plagioclase is used in this study for convenience.

Maskelynite (i.e., diaplectic glass with plagioclase composition) and melt-quenched amorphous plagioclase can be distinguished depending upon their formation mechanisms. Diaplectic maskelynite is formed by a solid-state transition under instant, high-pressure during shock events (Stöffler & Hornemann, 1972). The high strain rate and pressure, as well as high temperature, under shocked condition of 28–37 GPa can lead to the vitrification of plagioclase without melting, and with an accompanying increase in the coordination of silicon and aluminum atoms in diaplectic glass (Williams & Jeanloz, 1989). Diaplectic glass can be formed at lower temperatures than the melting point because the melting phase is not necessary for its formation. Shock temperature also plays an important role in the formation of diaplectic glass. The amorphization pressure of diaplectic glass decreases as temperatures increase (Kubo et al., 2010). For instance, labradorite is amorphized under ~37 GPa at room temperature, but ~31 GPa at 270 °C (Tomioka et al., 2010). Meanwhile, melt-quenched amorphous plagioclase is also formed by the quenching of dense plagioclase melts under shocked conditions at high temperature and pressure. Thus, shock temperature should be higher than the melting point at the shock pressure for the melting of plagioclase to occur. In short, high pressure plays a more important role than temperature for diaplectic glass, whereas high temperatures above the melting point are important in the formation of melt-quenched amorphous plagioclase.

In order to infer shock conditions using amorphous plagioclase, the glass type should be determined first because diaplectic and melt-quenched glasses are formed by pressure-induced and thermally induced amorphization, respectively. To date, they have been distinguished primarily by observing differences in their morphological features obtained through imaging using, for example, optical and electron microscopes. The morphological differences between these two types of amorphous plagioclase are essentially based on the rheological difference of solids and liquids. Diaplectic glass generally can be recognized by its morphological characteristics, such as pseudomorphic grain shapes of original minerals, isotropic and glassy textures, and monomineralic composition (French & Koeberl, 2010). Melt-quenched amorphous plagioclase can also be identified by the presence of microflows, offshoot structures, expansion cracks, and a smooth surface (Chen & El Goresy, 2000).

Previous attempts to determine the different formation mechanisms of the two types of amorphous plagioclase have also been made using various spectrometers, including Raman spectroscopy, solid-state nuclear magnetic resonance, and high-energy X-ray total scattering (Fritz et al., 2005; Jaret et al., 2015). Raman spectra provide the degree of amorphization based on the widths and intensities of symmetrical stretching bands of T-O-T (where T = Si or Al tetrahedra) and lattice vibrational bands (Heymann & Hörz, 1990). With these advantages, Raman spectroscopy has been successfully used to estimate the shock pressure of plagioclase and maskelynite in meteorites (Fritz et al., 2005), but no significant differences depending on the formation mechanism of amorphous plagioclase have been observed convincingly without the use of a multitechnique approach (Jaret et al., 2015).

As one of the solid-solution minerals, plagioclase exhibits compositional variation, which affects melting temperature and solid-state amorphization pressure. Thus, a chemical approach is necessary and could provide the essential clues needed to distinguish between the two types of amorphous plagioclase. The chemical composition of diaplectic maskelynite rarely changes from preshocked plagioclase (Jaret et al., 2015; Pickersgill et al., 2015). Even the chemical zoning is preserved in diaplectic maskelynite (Jaret et al., 2015). Interestingly, the chemical composition of plagioclase is known to affect the amorphization pressure of maskelynite. With an increasing albite (Ab) ratio in plagioclase, the amorphization pressure also increases (Stöffler et al., 1986). The amorphization pressure for labradorite and albite has been measured as ~22 and ~33 GPa, respectively (Heymann & Hörz, 1990; Kubo et al., 2010). In short, the chemical composition of plagioclase affects pressure-induced amorphization conditions, but such amorphization does not lead to variations in its chemical composition.

For melt-quenched amorphous plagioclase, chemical differences between amorphous and crystalline plagioclase have been reported for many meteorites. A lack of potassium and nonstoichiometric composition occur as a result of melting and subsequent quenching (Chen & El Goresy, 2000); however, the mechanism of this chemical variation has not yet been clarified. Additionally, most studies have focused on albite and oligoclase and not anorthite (An). Here we explore partially amorphized plagioclase grains in the lunar meteorite by analyzing their textures, atomic-scale structures, and chemical compositions. The objective of this study is to provide the chemical evidence necessary to distinguish the formation mechanism of a partial amorphous phase in shock plagioclase.

2. Materials and Methods

2.1. Samples

Mount DeWitt (DEW) 12007 is a lunar meteorite found in Antarctica during the joint expedition of South Korea and Italy in the 2012–2013 field season. It consists of plagioclase-rich clasts containing 50–75 vol % of calcic plagioclase (An_{>85}) as well as pigeonite, augite, and minor phases of ilmenite, baddeleyite, and tiny grains of Fe,Ni metal. Details of the mineralogy, petrography, and oxygen isotopic composition of meteorite DEW 12007 were reported in previous studies (Collareta et al., 2016; Han, 2016).

2.2. Analytical Methods

The occurrence of partially amorphized plagioclase grains in DEW 12007 was observed using a polarized optical microscope. Polished thin sections of DEW 12007 were coated with approximately 25 nm of thick carbon film for electron microprobe analysis. Mineral chemistry and backscattered electron (BSE) images were obtained with a field emission electron probe microanalyzer (FE-EPMA; JEOL JXA-8530F, Japan) at the Korea Polar Research Institute using a 15-keV accelerating voltage, 20-nA beam current, and a beam size of ~1 μm with five wavelength-dispersive X-ray spectrometers. Natural and synthetic mineral standards from the Smithsonian and JEOL, including albite, rutile, jadeite, Cr₂O₃, fayalite, MnO, MgO, wollastonite, and microcline, were used as standards. The counting time on peaks was 20 s, and the mean atomic number was used to correct for background and matrix effects (Donovan & Tingle, 1996) using an improved mean atomic number background correction for quantitative microanalyses. X-ray elemental maps of plagioclase grains were obtained using the EPMA system with a focused beam at a 100-nA beam current, dwell time of 50 ms, and step size of 1 μm. The maps were converted to quantitative elemental maps using Probe Image software (Probe Software, USA). Cathodoluminescence (CL) images were obtained using MiniCL (Gatan, USA) attached to a scanning electron microscope (JEOL JSM 6610) at the Korea Polar Research Institute with 15 keV. Micro-Raman spectra were obtained using a LabRAM HR UV/VIS/NIR (Horiba Scientific, Japan) with a He-Ne laser at a 632-nm wavelength and 400-mW power. The Raman spectra were collected from 200 to 1,800 cm⁻¹ with a spot size of ~1 μm. Spectra were compiled after seven scans with a collecting time of 10 s. Raman two-dimensional mapping images consisted of 40 × 71 grids with interval of 4 μm. Each intensity of points was obtained by the integration of Raman peaks ranging from 420 to 600 cm⁻¹.

3. Results

3.1. Optical Microscopic Analysis

Figure 1 shows the polarized optical microscopic images of partially amorphized plagioclase grains in meteorite DEW 12007. Crystalline and amorphous plagioclases are clearly distinguishable due to the optical extinction of amorphous phase in cross-polarized light (XPL) images. Most plagioclase grains have been partially transformed to amorphous phase. The degree of amorphization (i.e., fraction of amorphous regions in a grain) varies grain by grain. In this study, we designated the crystalline and amorphous phase in partially amorphized plagioclase grains as “crystalline regions” and “amorphous regions” to discriminate them from whole crystalline or amorphous grains.

An interesting feature of the partially amorphized plagioclase in DEW 12007 is its apparent directionality (Kim & Park, 2016), possibly due to the direction of the predominant impact event. Although the partial amorphization of plagioclase is rather common (Chen & El Goresy, 2000; El Goresy et al., 2013; Liu et al., 2009; Takeda et al., 1993; Van Schmus & Ribbe, 1968), such directionality in amorphization has not been reported before. It is difficult to know precisely why there is a directionality in the amorphization of

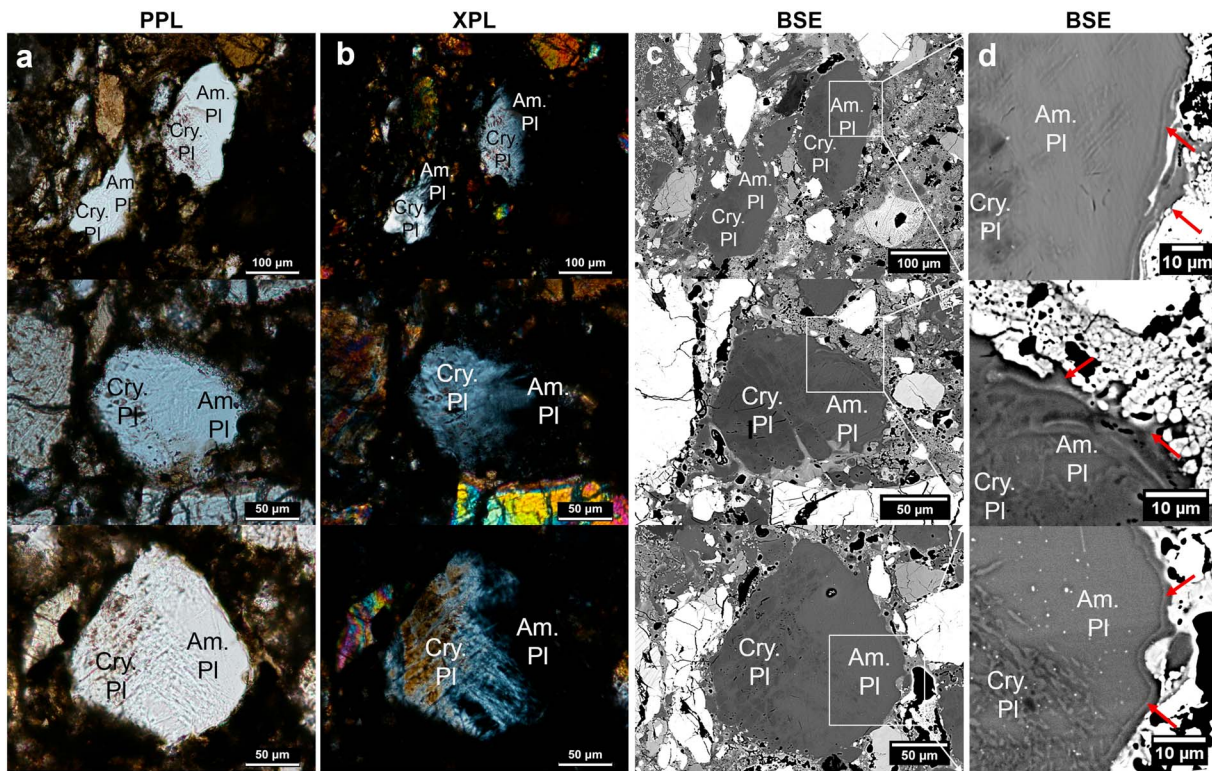


Figure 1. (a) Optical microscopic plain polarized light (PPL), (b) cross-polarized light (XPL) and (c) backscattered electron (BSE) images of partially amorphized plagioclase in the lunar meteorite DEW 12007. (d) Enlarged images of the boxed regions shown in BSE images. Modified from Kim and Park (2016) with permission from the Journal of the Mineralogical Society of Korea. Cry. PI and Am. PI indicates the crystalline plagioclase and amorphous plagioclase, respectively.

plagioclase in DEW 12007, but it is probably related to either the location of shock veins or the direction of impact. The deformational and thermal conditions associated with shock compression can be notably inhomogeneous (Arndt et al., 1982), which may lead to inhomogeneous amorphization. Otherwise, it may be due to the heterogeneity in brecciated meteorites.

Backscattered electron images in Figure 1d show the detailed textures of partially amorphized plagioclase grains in DEW 12007. The reliefs of preexisting cracks were observed in crystalline regions, while a smooth texture was obvious in amorphous regions. Microflow structures and recrystallized phases were observed along the boundaries between amorphous region and the nearby matrix (arrows in Figure 1d). The grains generally showed pseudomorphic textures of the preshocked plagioclase grains, although some microflows also infiltrated into the nearby matrix.

3.2. Raman Spectroscopic Results

Figure 2 shows the Raman spectrum measured along the diagonal path of a partially amorphized plagioclase grain. Raman spectroscopy was performed along the arrows shown in XPL (Figure 2a) and BSE (Figure 2b) images, and the measurement spot was marked by the distance from the point where the arrow began. As shown in the XPL and BSE images, approximately two thirds of the arrow corresponded to the crystalline region (~0–200 μm), and one third of the end of the arrow corresponded to the amorphous region (~200–300 μm). Additionally, the amorphous region was extinguished in the XPL image and showed a smooth texture in the BSE image. The crystalline region revealed strong Raman peaks at 390, 480, 500, and 550 cm^{-1} , which are typical bands for shocked plagioclase at ~5–32 GPa (Fritz et al., 2005; Kayama et al., 2009). In the amorphous region, Raman peaks broadened substantially, ranging from 460 to 600 cm^{-1} , with low heights due to the disordered atomic structure (Kim & Park, 2016).

We obtained two-dimensional Raman mapping images with peak intensities between 420 and 600 cm^{-1} with a symmetrical stretching of T-O-T, where T represents Si or Al tetrahedra, and compared them with XPL, BSE, and CL images as shown in Figure 3. Due to the loss of periodicity in atomic arrangement

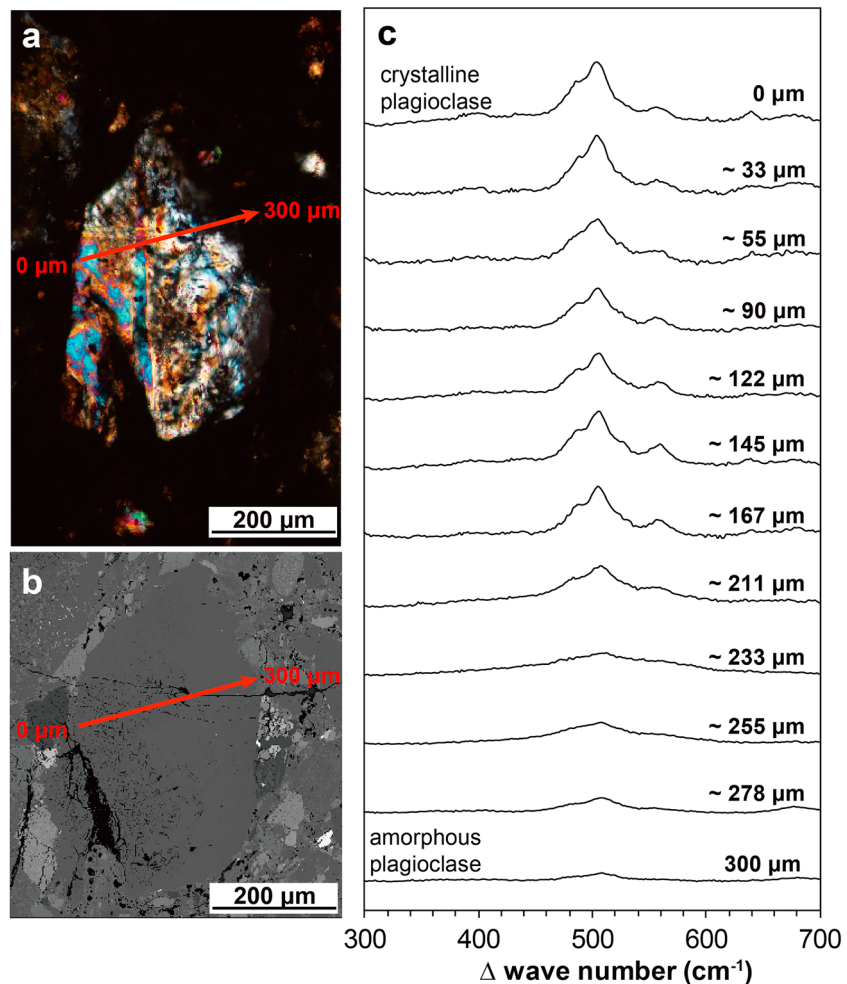


Figure 2. (a) Optical microscopic XPL and (b) BSE image of a partially amorphized plagioclase grain in DEW 12007. (c) Raman spectra obtained with varying measurement points along the red arrows in XPL (a) and BSE image (b) from the crystalline region to the amorphous region.

during amorphization, the relative peak intensities represent the degree of crystallinity. The maximum and minimum peak intensities between 420 and 600 cm^{-1} were normalized from 1 to 0. The lower peak intensities indicated a more disordered state (i.e., amorphous plagioclase). The mapping images were quite similar to the XPL and BSE images, indicating that the degree of amorphization was well reflected in the mapping images. The boundaries between crystalline and amorphous regions show relatively sharp transitions, rather than gradual. Raman spectra allowed us to confirm the disordered structure of the amorphous region, but could not provide the essential clues need to determine the amorphization mechanism (i.e., melt quenched glass versus diaplectic glass).

3.3. Cathodoluminescence Analysis

Cathodoluminescence is one of the most efficient methods of observing crystal growth and metamorphic textures in minerals, as the intensity varies depending upon crystal lattice defects and the composition of trace elements (Gucsik et al., 2003; Hamers & Drury, 2011; Kayama et al., 2009; Mora & Ramseier, 1992). The CL images of partially amorphized plagioclase grains in Figures 3 and 4 show slightly brighter CL signals from amorphous regions than from crystalline regions. Kato et al. (2017) also reported CL images where the bright and dark portions correspond to maskelynite and plagioclase, respectively. The microscopic origin of the brighter luminescence of amorphous plagioclase relative to the crystalline plagioclase in DEW 12007 may due to structural disordering, but it may also be due to a chemical difference between them, such as the relative abundances of Na, Ca, and Fe (Masahiro et al., 2018).

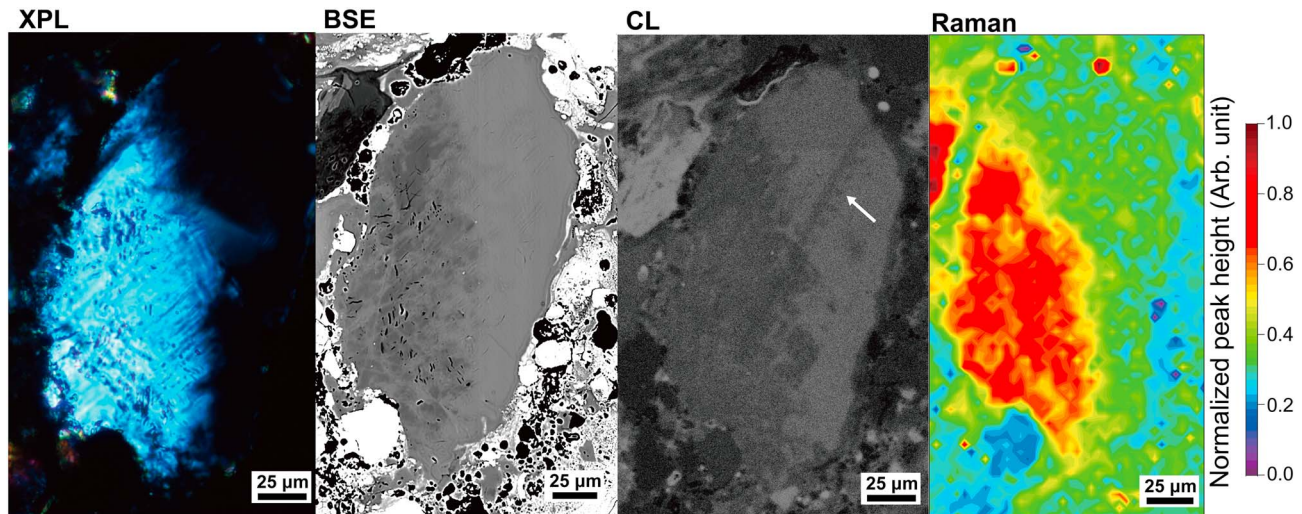


Figure 3. Comparison of imaging analysis methods including XPL, BSE, cathode luminescence (CL), and Raman imaging from left to right. In the CL image, light gray corresponds to more luminous regions and the straight line (arrow) indicates the damage from EPMA. In the Raman image, peak intensities between 460 and 600 cm^{-1} were normalized from 1 (maximum intensity) to 0 (minimum intensity).

Figure 4 shows the comparison of BSE and CL images of partially amorphized plagioclase grains. The BSE images show smooth textures in amorphous regions and cracks inside of crystalline regions. The distribution of smooth textures in BSE images is remarkably similar to that of luminescence in the CL images. These results indicate that the amorphization of plagioclase likely initiates from cracks during shock. The melting of plagioclase is known to initiate from the surface and cracks by thermal heating (Tsuchiyama & Takahashi, 1983). Thus, the amorphous phase along the cracks of plagioclase indirectly supports the conclusion that the amorphous region in plagioclase from DEW 12007 is a normal glass quenched from melts, rather than a diaplectic glass.

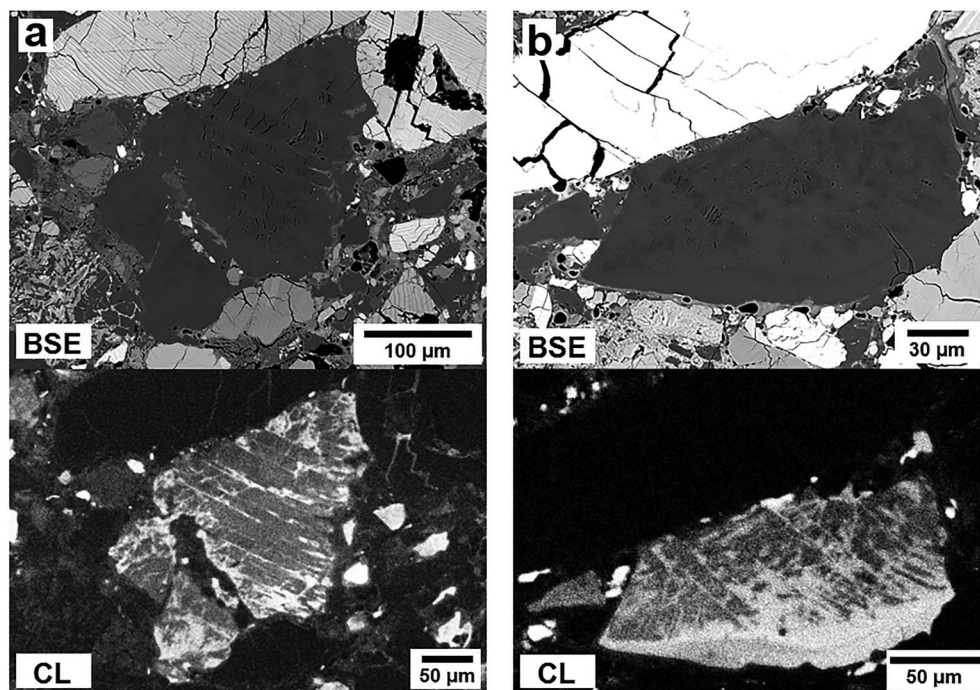


Figure 4. Comparison between (top) BSE and (bottom) CL images of partially amorphized plagioclase grains. The amorphous plagioclase region with a smooth texture in the BSE images coincides with the luminous region in CL images.

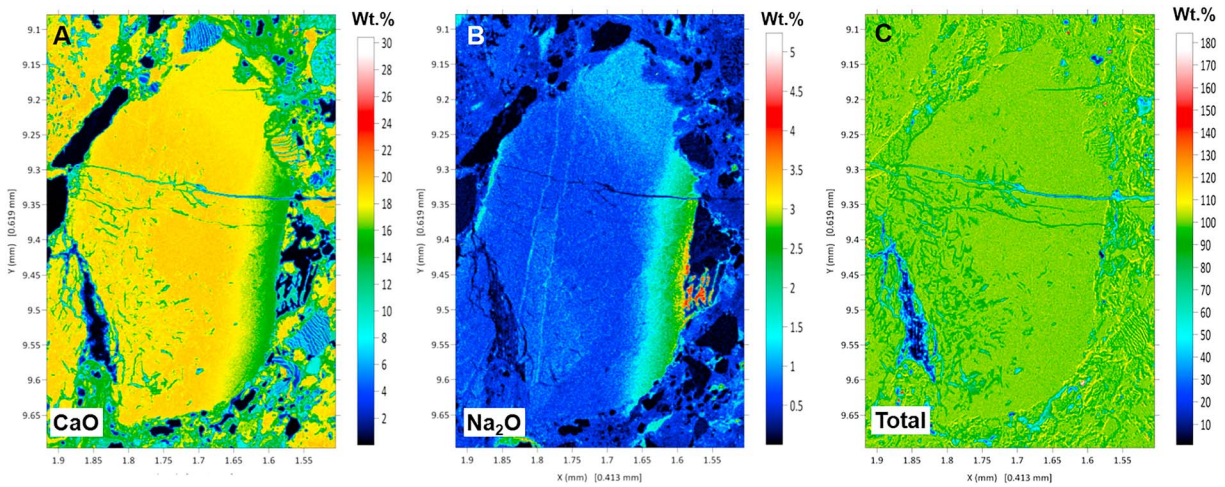


Figure 5. CaO, Na₂O, and K₂O wt% obtained from X-ray maps in (a) Ca K α , (b) Na K α , and (c) K K α of partially amorphized plagioclase grain. The BSE image and EPMA results of the grain is presented in Figure 2 and Table 1, respectively.

3.4. EPMA and Energy-Dispersive X-ray Spectroscopy

Quantitative maps of CaO, Na₂O, and K₂O (wt %) shown in Figure 5 reveal the heterogeneous distribution of chemical compositions in the partially amorphized plagioclase of DEW 12007. The Ca, Na, and K contents differed between crystalline and amorphous regions in each grain. In general, enrichments of Na and K in the amorphous region were observed. The chemical composition was relatively uniform in the crystalline regions, but it gradually changed in amorphous regions away from the crystalline-amorphous phase boundaries. The regions where chemical variations occurred corresponded well with the places where amorphization occurred. As the degree of amorphization increased, the content of Na and K also increased.

In order to investigate the effects of chemical composition on the amorphization of shocked plagioclase and vice versa, we quantitatively analyzed the chemical compositions of crystalline and amorphous plagioclase using an EPMA. The detailed results are shown in Table 1 and in the supporting information. The numbers of Ca and Na, on the basis of eight oxygens in crystalline plagioclase region, were approximately 0.94 and 0.06, respectively, which agrees with previous a report on the composition of plagioclase (Ab₀₈An₉₂) in DEW 12007 (Collareta et al., 2016). The amorphous plagioclase regions showed higher Na contents than those of crystalline regions, although Na contents varied among grains.

Table 1

Selected Electron Probe Microanalyzer (EPMA) Results of Crystalline Plagioclase (Cry. Pl) and Amorphous Plagioclase (Am. Pl) Regions in the Meteorite DEW 12007

Composition of oxides (wt %)

		Na ₂ O	MgO	SiO ₂	Al ₂ O ₃	K ₂ O	CaO	FeO	MnO	Cr ₂ O	TiO ₂	Total
Grain 1 ^a	Cry. Pl	0.67	0.04	44.82	34.55	0.05	18.63	0.30	0.03	0.00	0.02	99.09
	Am. Pl	2.19	0.12	49.61	31.88	0.33	15.37	0.86	0.02	0.00	0.04	100.42
Grain 2 ^b	Cry. Pl	1.10	0.07	45.76	33.16	0.07	17.94	0.39	0.01	0.04	0.04	98.59
	Am. Pl	1.88	0.07	47.89	32.46	0.18	16.42	0.63	0.00	0.00	0.03	99.56
Number of cations (oxygens) = 8												
		Na	Mg	Si	Al	K	Ca	Fe	Mn	Cr	Ti	Total
Grain 1 ^a	Cry. Pl	0.060	0.003	2.088	1.897	0.003	0.930	0.012	0.001	0.000	0.001	4.994
	Am. Pl	0.193	0.008	2.263	1.714	0.019	0.752	0.033	0.001	0.000	0.001	4.985
Grain 2 ^b	Cry. Pl	0.100	0.005	2.140	1.828	0.004	0.899	0.015	0.000	0.002	0.002	4.996
	Am. Pl	0.168	0.005	2.210	1.765	0.011	0.812	0.024	0.000	0.000	0.001	4.996

^aGrain 1 is shown in Figures 2 and 5. ^bGrain 2 is shown in Figure S1 in the supporting information.

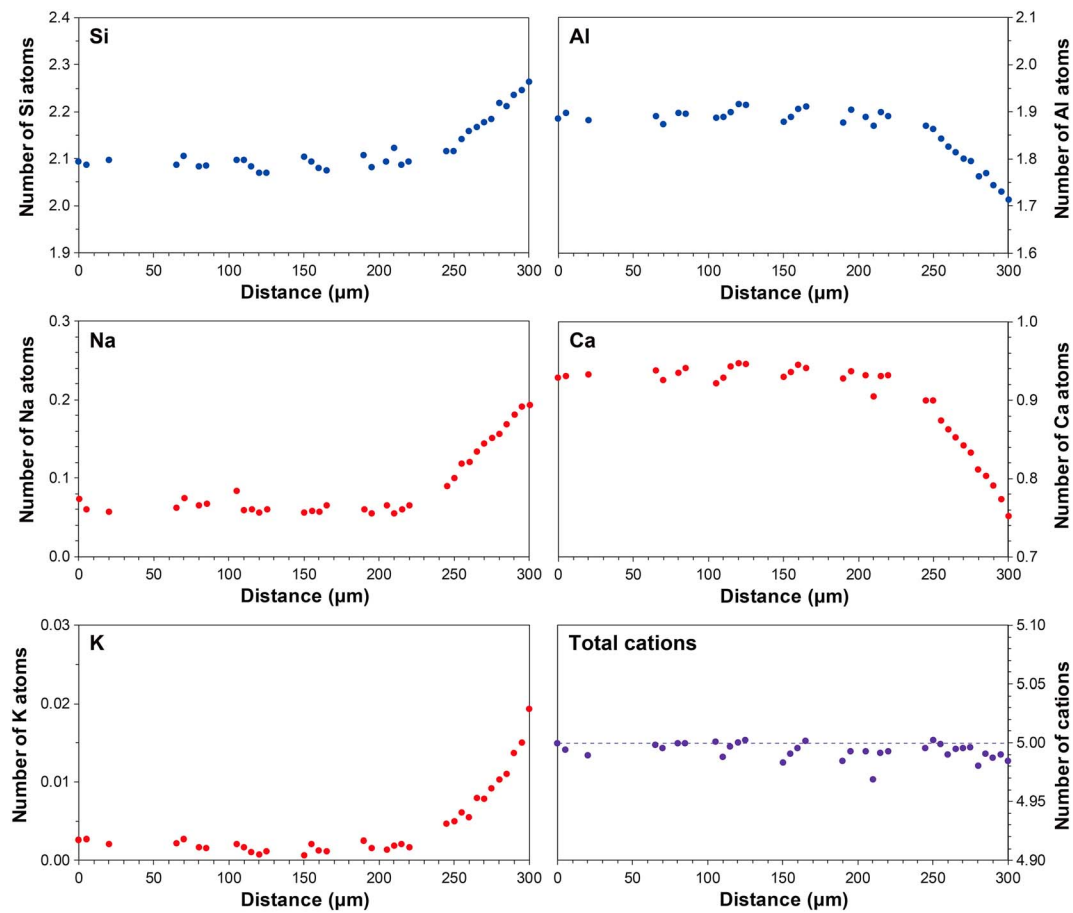


Figure 6. Compositional profiles for partially amorphized plagioclase grains. The y axis indicates the number of cations based on eight oxygens in the plagioclase composition.

Figure 6 shows that the variations in the number of cations, on the basis of eight oxygens along the line from the crystalline to the amorphous plagioclase region, were obtained from the same line used in Raman spectroscopy (Figure 2). The Ca content decreased while Na content increased as the measuring spot moved from the crystalline region to the amorphous region. The number of Na and Ca atoms per eight oxygens in the amorphous region reached a maximum of 0.2 and a minimum of 0.75, respectively. The number of K atoms also increased from 0.002 in the crystalline region up to 0.02 in the amorphous region. The concentrations of Al and Si also varied due to coupled substitution with Ca and Na, respectively, in plagioclase. These results support the conclusion that the difference in chemical compositions between crystalline and amorphous regions was slight but clear. We also noted that not all partially amorphized plagioclase grains showed substantial differences in the compositions of crystalline and amorphous regions. Several grains often showed trivial variations in chemical composition between these two regions in DEW 12007 (Figure S1) but exhibited the same chemical trends as those described above.

The different chemical compositions of melt-quenched amorphous plagioclase (i.e., normal glass-type maskelynite in the references) and crystalline plagioclase have been reported before (Bischoff et al., 2013; Chen & El Goresy, 2000; Kato et al., 2017), but the results of such studies were somewhat different from those presented here. The meteorites Peace River, Tenham, Dar al Gani 355, and Yamato 790729 show higher K and lower Na concentrations in melt-quenched amorphous plagioclase than in crystalline plagioclase, and the number of cations also deviates from stoichiometry (Chen & El Goresy, 2000; Gillet et al., 2000; Kato et al., 2011). Meanwhile, in DEW 12007, both the K and Na concentrations are higher in amorphous region than in crystalline regions. The K content of amorphous plagioclase linearly increased with the ratio of ~ 0.1 with Na content as the crystalline phase transformed to amorphous phase (Figure 7). The number of cations also did not significantly deviate from the stoichiometry of ideal plagioclase in either the crystalline or

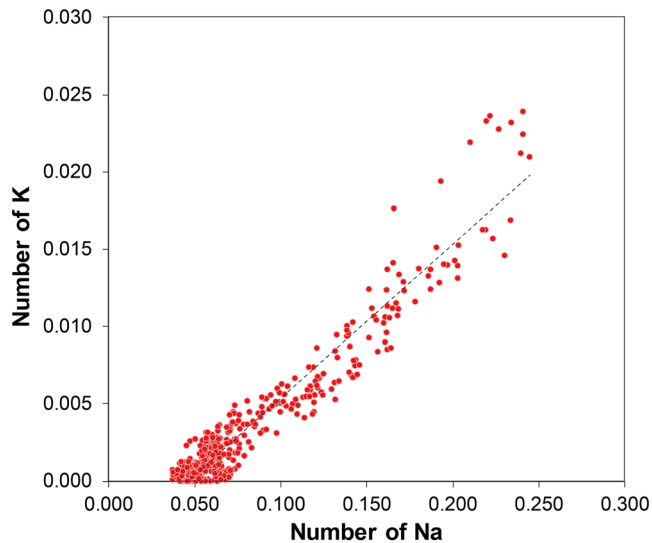


Figure 7. Linear correlation between the atomic numbers of Na and K in partially amorphized plagioclase grains in DEW 12007.

amorphous regions (Figure 6). During the EPMA measurements, Na in an amorphous phase could be selectively lost, resulting in deviation from stoichiometry of plagioclase (Mikouchi et al., 1999). However, in this study, Na increased in amorphous regions. Thus, the variation in the chemical composition of amorphous plagioclase in DEW 12007 was distinct from the nonstoichiometric compositions that were previously reported for other meteorites (Chen & El Goresy, 2000; Kato et al., 2011). Although crystalline and amorphous plagioclase have different chemical compositions, each of them occurred in stoichiometric balance in DEW 12007.

4. Discussion

In this study, we investigated the atomic-scale structures and chemical compositions of partially amorphized plagioclase in the lunar meteorite DEW 12007. Morphological characteristics of partial melting were observed in partially amorphized plagioclase grains. As shown in Figure 8, chemical variations and structural changes were well-correlated, indicating that amorphization induced the chemical changes or vice versa.

Considering the nature of the partial melting of plagioclase, the chemical differences between crystalline and amorphous plagioclase can provide valuable clues into its formation mechanism. It is well known that the partial melting of plagioclase induces chemical differences between solids and melts due to their different solidus and liquidus temperatures (Johannes et al., 1994; Tsuchiyama & Takahashi, 1983). Under ambient pressure, Ab-rich melts and An-rich solid phases (i.e., yet unmelted plagioclase) are observed as a result of the partial melting of plagioclase. The phase relationships of plagioclase under several tens of gigapascals are, unfortunately, poorly understood. The solidi of albite and anorthite have been reported only up to 3 and 1 GPa, respectively, which correspond to ~1,360 and ~1,570 °C (Boettcher et al., 1982; Boettcher et al., 1984; Boyd & England, 1963; Goldsmith, 1980). At both 1 atm and 1 GPa, the solidus of anorthite is approximately 350–380 °C higher than that of albite (Boettcher et al., 1982; Boettcher et al., 1984; Boyd & England, 1963; Goldsmith, 1980). Under the assumption that the phase relationships of plagioclase under several tens of gigapascals would have similar behaviors with those under ambient pressure, the chemical differences between the amorphous and crystalline plagioclase regions in DEW 12007 can be explained by partial melting within a shocked environment. If the amorphous plagioclase was formed via partial melting and subsequent quenching, the Na concentration of amorphous regions would be higher than that of crystalline regions in partially molten, individual grains.

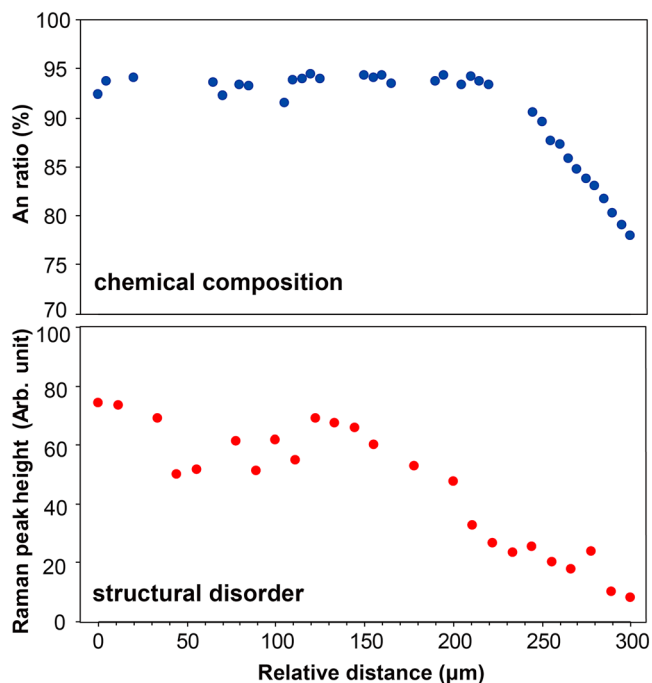


Figure 8. Variation in the chemical composition and structural disorder in the partially amorphized plagioclase grain shown in Figure 2. Chemical composition and structural disorder were calculated from EPMA and Raman spectroscopy results and are shown in percentages and arbitrary units, respectively.

As shown in the EPMA results, the amorphous plagioclase regions show higher Na, K, Fe, and Mg and lower Ca contents in comparison to the crystalline regions in DEW 12007 (Figure 6). The chemical evolution from crystalline to amorphous plagioclase regions corresponds well with its formation mechanism (i.e., partial melting and subsequent quenching). The higher Na and K contents in amorphous plagioclase may be due to the underlying phase relationships of plagioclase, which are frequently observed in partial melts of plagioclase at 1 atm of pressure (Currie, 1971; Johannes et al., 1994; Smith & Parsons, 1974; Tsuchiyama & Takahashi, 1983). A higher Fe content in melts has also been experimentally shown during the partial melting of plagioclase (Johannes et al., 1994). It is also worth noting that melt-quenched amorphous plagioclase reflects the composition of a melt.

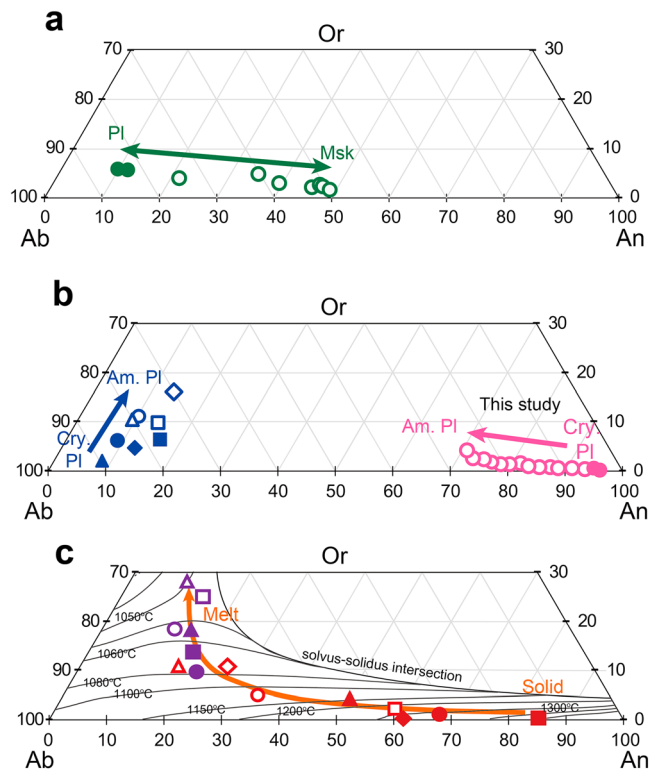


Figure 9. Chemical composition of crystalline and amorphous plagioclase depending on the formation mechanism of amorphous plagioclase. (a) Maskelynite is formed by pressure-induced amorphization (i.e., formation of diaplectic glass), green open circle (Bischoff et al., 2013). (b) Amorphous plagioclase is formed by partial melting (i.e., formation of normal glass), pink solid circle (this study); blue solid and open symbols correspond to crystalline and melt-quenched amorphous plagioclase, respectively (Chen & El Goresy, 2000). (c) Chemical difference between solid and melts during partial melting of plagioclase by heating at ambient pressure or $P_{H_2O} = 0.5$ kbar; red solid and open symbols correspond to solid and melts in partially molten, An-rich plagioclase (Smith & Parsons, 1974); purple solid and open symbols correspond to solid and melts in partially molten, Ab-rich alkali-feldspar (Morse, 2017); and black and gray lines show the solvus-solidus intersection and solidus lines for feldspar, respectively (Morse, 2017).

Here we propose two scenarios wherein the chemical differences between crystalline and amorphous regions were observed in a partially amorphized plagioclase grain. The first scenario is that chemically controlled amorphization occurred in a chemically heterogeneous plagioclase under shocked conditions (Bischoff et al., 2013; Stöffler et al., 1986). Chemical heterogeneities in preshocked plagioclase grains can lead to partial amorphization. This is because temperature and pressure conditions at which amorphization occurs depending on the composition of plagioclase. For instance, the amorphization pressure for plagioclase decreases with increasing An composition in diaplectic glass (Heymann & Hörz, 1990; Kubo et al., 2010; Stöffler et al., 1986). Thus, under specific shock pressures, relatively An-rich maskelynite and Ab-rich plagioclases could coexist as a result of partial amorphization. Bischoff et al. (2013) reported the “compositionally controlled transformation of plagioclase into maskelynite by shock,” as shown in Figure 9a. The coexistence of maskelynite with An_{10} and plagioclases with An_{50-52} was observed in the Villalbeto de la Pena meteorite (Bischoff et al., 2013). Strictly speaking, the case reported by Bischoff et al. (2013) did not involve the partial amorphization of individual grains. The maskelynite in their study was a preexisting An_{50-52} plagioclase inclusion in an An_{10} matrix. During the shock event, the inclusion was transformed into maskelynite, while the matrix remained a crystalline plagioclase (Bischoff et al., 2013). Indeed, a chemical evolution of partially amorphized diaplectic glass-type maskelynite has not yet been observed to our knowledge (Pickersgill et al., 2015).

The second scenario we present here is that of partial melting-induced chemical differences between crystalline and amorphous plagioclase, which have been reported in melt-quenched amorphous plagioclase (normal glass-type maskelynite in the reference; Chen & El Goresy, 2000). While preshocked plagioclase grains are chemically homogeneous, partial melting under shocked conditions causes the chemical difference between melts and solids to evolve. We again noted that this was the case for partially amorphized plagioclase grains. Figure 9b shows the chemical evolution of crystalline and melt-quenched amorphous plagioclase as a result of partial melting. For amorphous plagioclase formed by partial melting of anorthite-rich feldspar, albite and orthoclase (Or) compositions are richer in amorphous regions than crystalline regions, which is the case for DEW 12007 (pink symbols in Figure 9b). Meanwhile, melt-quenched amorphous plagioclase formed by the partial melting of albite-rich feldspar shows a reduction in Na content in other meteorites previously reported. For instance, the plagioclase and melt-quenched amorphous plagioclase in the Peace River meteorite have composition of $Or_5Ab_{82}An_{13}$ and $Or_{16}Ab_{70}An_{14}$, respectively (blue triangles in Figure 9b; Chen & El Goresy, 2000). At a glance, these results may seem to contradict our results, but it is reasonable for the partial melting of oligoclase and albite to lead to K-rich melts, considering the phase relationships of alkali-feldspar (Morse, 2017; Smith & Parsons, 1974).

The chemical evolution of partially molten plagioclase at ambient pressure is shown in Figure 9c. In general, partial melting of An_{50-90} plagioclase leads to substantial increases in the Ab contents of melts, as well as slight increases in Or content (red symbols in Figure 9c; Smith & Parsons, 1974). For partially molten An_{10-20} plagioclase, the Or content clearly increases in melts in comparison to solids (purple symbols; Morse, 2017). Although the melting pressures differ, the tendency for chemical changes in the melt-quenched amorphous plagioclase under shock pressure shown in Figure 9b and plagioclase melts formed by partial melting at 1 atm are quite similar. No previous studies have reported on the compositional changes of plagioclase due to partial melting at several tens of gigapascals; however, the melt-quenched amorphous

plagioclase observed in this meteorite may provide insights into such changes. The alteration of chemical composition by amorphization is a feature that can be observed only in melt-quenched amorphous plagioclase. For maskelynite, it is difficult to induce chemical differences between amorphous and crystalline plagioclase regions through solid-state amorphization, as diaplectic glass preserves the chemical composition and texture of the original mineral (Jaret et al., 2015; Pickersgill et al., 2015).

The chemical differences between crystalline and amorphous regions in partially amorphized plagioclase grains may reveal the hidden formation mechanism (i.e., whether it was formed by a solid-state transition or by melting and subsequent quenching). It is difficult to induce chemical differences between crystalline and amorphous regions via solid-state amorphization. However, if amorphous plagioclase was formed by partial melting, specific cations should be enriched in melts, depending on their phase relationships for a specific pressure, temperature, and chemical composition of plagioclase. Thus, the appearance of partially amorphized plagioclase can bracket the pressure and temperature conditions along the solid-liquid transition. Unfortunately, phase diagrams (and the transitions they represent) with varying pressures, temperatures, and chemical compositions of plagioclase are poorly understood. Thus, in order to utilize the chemical composition of amorphous plagioclase in meteorites to index the pressure and temperature of shock events, an investigation of the phase relationships of plagioclase under high-pressure is necessary.

5. Conclusions

In the lunar meteorite DEW 12007, part of each plagioclase grain was transformed into an amorphous phase, and thus, crystalline and amorphous regions coexist in each individual grain. Amorphous plagioclase shows the characteristics of a glass quenched from a melt, such as smooth surfaces, microflow textures, and recrystallization bands. Cathodoluminescence images show that amorphous plagioclase exists along the preexisting cracks developed inside of crystalline regions, which is generally observed during the partial melting of plagioclase. In DEW 12007, compositional differences between crystalline region ($\text{Ab}_{08}\text{An}_{92}$) and amorphous region ($\text{Or}_{02}\text{Ab}_{28}\text{An}_{70}$) indicate that the amorphization process induced chemical variation or vice versa. Higher Ab contents in amorphous region relative to crystalline region can be observed during partial melting if the phase relationships of plagioclase under shock pressures are similar to those at ambient pressure. In this case, partial amorphization leads to chemical differences between crystalline and amorphous plagioclase. Meanwhile, if plagioclase grains are partially amorphized into diaplectic maskelynite, the chemical composition should not change. The chemical heterogeneity of plagioclase controls the glass type of amorphous plagioclase under shock pressures. The results of this study can provide insights into the identification of the formation mechanism of amorphous plagioclase including maskelynite and melt-quenched glass in partially amorphized plagioclase grains.

Acknowledgments

This work was supported by the National Research Foundation of Korea (grant NRF-2016R1C1B1010108), the Korea Polar Research Institute Project PE19230, and “Human Resources Program in Energy Technology” of the Korea Institute of Energy Technology Evaluation and Planning (KETEP) granted financial resource from the Ministry of Trade, Industry and Energy, Republic of Korea (20194010201730). The raw data are available on the website of Korea Polar Data Center (entry ID: KOPRI-KOREAMET-00000066; <https://dx.doi.org/doi:10.22663/KOPRI-KOREAMET-00000066.4>). We thank L. Montesi, A. Rogers, S.A. Morse, S.J. Jaret, and anonymous reviewer for their critical and helpful comments on the manuscript. Conflict of Interest: None.

References

- Arndt, J., Hummel, W., & Gonzalez-Cabeza, I. (1982). Diaplectic labradorite glass from the Manicouagan impact crater. *Physics and Chemistry of Minerals*, 8(5), 230–239. <https://doi.org/10.1007/BF00309482>
- Bischoff, A., Dyl, K. A., Horstmann, M., Ziegler, K., Wimmer, K., & Young, E. D. (2013). Reclassification of Villalbeta de la Peña—Occurrence of a winonaite-related fragment in a hydrothermally metamorphosed polymict L-chondritic breccia. *Meteoritics and Planetary Science*, 48(4), 628–640. <https://doi.org/10.1111/maps.12076>
- Boettcher, A., Guo, Q., Bohlen, S., & Hanson, B. (1984). Melting in feldspar-bearing systems to high pressures and the structures of aluminosilicate liquids. *Geology*, 12(4), 202–204. [https://doi.org/10.1130/0091-7613\(1984\)12<202:mifsth>2.0.co;2](https://doi.org/10.1130/0091-7613(1984)12<202:mifsth>2.0.co;2)
- Boettcher, A. L., Burnham, C. W., Windom, K. E., & Bohlen, S. R. (1982). Liquids, glasses, and the melting of silicates to high pressures. *Journal of Geology*, 90(2), 127–138. <https://doi.org/10.1086/628658>
- Boyd, F. R., & England, J. L. (1963). Effect of pressure on the melting of diopside, $\text{CaMgSi}_2\text{O}_6$, and albite, $\text{NaAlSi}_3\text{O}_8$, in the range up to 50 kilobars. *Journal of Geophysical Research*, 68(1), 311–323. <https://doi.org/10.1029/JZ068i001p00311>
- Chen, M., & El Goresy, A. (2000). The nature of maskelynite in shocked meteorites: Not diaplectic glass but a glass quenched from shock-induced dense melt at high pressures. *Earth and Planetary Science Letters*, 179(3–4), 489–502. [https://doi.org/10.1016/S0012-821X\(00\)00130-8](https://doi.org/10.1016/S0012-821X(00)00130-8)
- Collareta, A., D’Orazio, M., Gemelli, M., Pack, A., & Folco, L. (2016). High crustal diversity preserved in the lunar meteorite Mount DeWitt 12007 (Victoria Land, Antarctica). *Meteoritics and Planetary Science*, 51(2), 351–371. <https://doi.org/10.1111/maps.12597>
- Currie, K. (1971). The composition of anomalous plagioclase glass and coexisting plagioclase from Mistastin Lake, Labrador, Canada. *Mineralogical Magazine*, 38(296), 511–517. <https://doi.org/10.1180/minmag.1971.038.296.14>
- Donovan, J. J., & Tingle, T. N. (1996). An improved mean atomic number background correction for quantitative microanalysis. *Microscopy and Microanalysis*, 2(1), 1–7. <https://doi.org/10.1017/S1431927696210013>
- El Goresy, A., Gillet, P., Miyahara, M., Ohtani, E., Ozawa, S., Beck, P., & Montagnac, G. (2013). Shock-induced deformation of Shergottites: Shock-pressures and perturbations of magmatic ages on Mars. *Geochimica et Cosmochimica Acta*, 101, 233–262. <https://doi.org/10.1016/j.gca.2012.10.002>

- French, B. M., & Koeberl, C. (2010). The convincing identification of terrestrial meteorite impact structures: What works, what doesn't, and why. *Earth-Science Reviews*, *98*(1-2), 123–170. <https://doi.org/10.1016/j.earscirev.2009.10.009>
- Fritz, J., Greshake, A., & Stöffler, D. (2005). Micro-Raman spectroscopy of plagioclase and maskelynite in Martian meteorites: Evidence of progressive shock metamorphism. *Antarctic Meteorite Research*, *18*, 96–116.
- Gillet, P., Chen, M., Dubrovinsky, L., & El Goresy, A. (2000). Natural NaAlSi₃O₈-hollandite in the shocked Sixiangkou meteorite. *Science*, *287*(5458), 1633–1636. <https://doi.org/10.1126/science.287.5458.1633>
- Goldsmith, J. R. (1980). The melting and breakdown reactions of anorthite at high pressures and temperatures. *American Mineralogist*, *65*(3-4), 272–284.
- Gucsik, A., Koeberl, C., Brandstätter, F., Libowitzky, E., & Reimold, W. U. (2003). Scanning electron microscopy, cathodoluminescence, and Raman spectroscopy of experimentally shock-metamorphosed quartzite. *Meteoritics and Planetary Science*, *38*(8), 1187–1197. <https://doi.org/10.1111/j.1945-5100.2003.tb00307.x>
- Hamers, M., & Drury, M. (2011). Scanning electron microscope-cathodoluminescence (SEM-CL) imaging of planar deformation features and tectonic deformation lamellae in quartz. *Meteoritics and Planetary Science*, *46*(12), 1814–1831. <https://doi.org/10.1111/j.1945-5100.2011.01295.x>
- Han, J. (2016). Petrography, geochemistry, and age of granophyre clast in the lunar meteorite DEW 12007, Yonsei University.
- Heymann, D., & Hörz, F. (1990). Raman-spectroscopy and X-ray diffractometer studies of experimentally produced diaplectic feldspar glass. *Physics and Chemistry of Minerals*, *17*(1), 38–44. <https://doi.org/10.1007/BF00209224>
- Jaret, S. J., Woerner, W. R., Phillips, B. L., Ehm, L., Nekvasil, H., Wright, S. P., & Glotch, T. D. (2015). Maskelynite formation via solid-state transformation: Evidence of infrared and X-ray anisotropy. *Journal of Geophysical Research: Planets*, *120*, 570–587. <https://doi.org/10.1002/2014JE004764>
- Johannes, W., Koepke, J., & Behrens, H. (1994). Partial melting reactions of plagioclases and plagioclase-bearing systems. In *Feldspars and their Reactions* (pp. 161–194). Dordrecht: Springer.
- Kato, Y., Sekine, T., Kayama, M., Miyahara, M., & Yamaguchi, A. (2017). High-pressure polymorphs in Yamato-790729 L6 chondrite and their significance for collisional conditions. *Meteoritics and Planetary Science*, *52*(12), 2570–2585. <https://doi.org/10.1111/maps.12957>
- Kato, Y., Sekine, T., & Yamaguchi, A. (2011). High pressure phases found in Yamato 790729, in *The 34th Antarctic Meteorite Symposium* edited, National Institute of Polar Research.
- Kayama, M., Gucsik, A., Nishido, H., Ninagawa, K., & Tsuchiyama, A. (2009). Cathodoluminescence and Raman spectroscopic characterization of experimentally shocked plagioclase. *AIP Conference Proceedings*, *1163*(1), 86–95. <https://doi.org/10.1063/1.3222897>
- Kim, H. N., & Park, C. (2016). Shock metamorphism of plagioclase-maskelynite in the lunar meteorite Mount DeWitt 12007. *Journal of the mineralogical society of Korea*, *29*(3), 131–139. <https://doi.org/10.9727/jmsk.2016.29.3.131>
- Kubo, T., Kimura, M., Kato, T., Nishi, M., Tominaga, A., Kikegawa, T., & Funakoshi, K.-i. (2010). Plagioclase breakdown as an indicator for shock conditions of meteorites. *Nature Geoscience*, *3*(1), 41–45. http://www.nature.com/ngeo/journal/v3/n1/supinfo/ngeo704_S1.html
- Liu, Y., Floss, C., Day, J. M. D., Hill, E., & Taylor, L. A. (2009). Petrogenesis of lunar mare basalt meteorite Miller Range 05035. *Meteoritics and Planetary Science*, *44*(2), 261–284. <https://doi.org/10.1111/j.1945-5100.2009.tb00733.x>
- Masahiro, K., Toshimori, S., Naotaka, T., Hirotsugu, N., Yukako, K., Kiyotaka, N., et al. (2018). Cathodoluminescence of high-pressure feldspar minerals as a shock barometer. *Meteoritics and Planetary Science*, *53*(7), 1476–1488. <https://doi.org/10.1111/maps.13092>
- Mikouchi, T., Miyamoto, M., & McKay, G. A. (1999). The role of undercooling in producing igneous zoning trends in pyroxenes and maskelynites among basaltic Martian meteorites. *Earth and Planetary Science Letters*, *173*(3), 235–256. [https://doi.org/10.1016/S0012-821X\(99\)00188-0](https://doi.org/10.1016/S0012-821X(99)00188-0)
- Mora, C. I., & Ramseyer, K. (1992). Cathodoluminescence of coexisting plagioclases, Boehls Butte anorthosite; CL activators and fluid flow paths. *American Mineralogist*, *77*(11-12), 1258–1265.
- Morse, S. A. (2017). Kiglapait mineralogy V: Feldspars in a hot, dry magma. *American Mineralogist*, *102*(10), 2084–2095. <https://doi.org/10.2138/am-2017-6098>
- Pickersgill, A. E., Osinski, G. R., & Flemming, R. L. (2015). Shock effects in plagioclase feldspar from the Mistastin Lake impact structure, Canada. *Meteoritics and Planetary Science*, *50*(9), 1546–1561. <https://doi.org/10.1111/maps.12495>
- Sims, M., Jaret, S. J., Carl, E., Rhymer, B., Schrodt, N., Mohrholz, V., et al. (2019). Pressure-induced amorphization in plagioclase feldspars: A time-resolved powder diffraction study during rapid compression. *Earth and Planetary Science Letters*, *507*, 166–174. <https://doi.org/10.1016/j.epsl.2018.11.038>
- Smith, P., & Parsons, I. (1974). The alkali-feldspar solvus at 1 kilobar water-vapour pressure. *Mineralogical Magazine*, *39*(307), 747–767. <https://doi.org/10.1180/minmag.1974.039.307.03>
- Stöffler, D., & Hornemann, U. (1972). Quartz and feldspar glasses produced by natural and experimental shock. *Meteoritics and Planetary Science*, *7*(3), 371–394. <https://doi.org/10.1111/j.1945-5100.1972.tb00449.x>
- Stöffler, D., Ostertag, R., Jammes, C., Pfannschmidt, G., Gupta, P. R. S., Simon, S. B., et al. (1986). Shock metamorphism and petrography of the Shergotty achondrite. *Geochimica et Cosmochimica Acta*, *50*(6), 889–903. [https://doi.org/10.1016/0016-7037\(86\)90371-6](https://doi.org/10.1016/0016-7037(86)90371-6)
- Takeda, H., Arai, T., & Saiki, K. (1993). Mineralogical studies of lunar meteorite Yamato-793169, a mare basalt. *Antarctic Meteorite Research*, *6*, 3–13.
- Tomioka, N., Kondo, H., Kunikata, A., & Nagai, T. (2010). Pressure-induced amorphization of albitic plagioclase in an externally heated diamond anvil cell. *Geophysical Research Letters*, *37*, L21301. <https://doi.org/10.1029/2010GL044221>
- Tschermak, G. (1872). Die Meteoriten von Shergotty und Gopalpur, Sitzber. Akad. Wiss. Wien Math.-Naturwiss. Kl. Abt. I, 65, 122–146.
- Tsuchiyama, A., & Takahashi, E. (1983). Melting kinetics of a plagioclase feldspar. *Contributions to Mineralogy and Petrology*, *84*(4), 345–354. <https://doi.org/10.1007/bf01160286>
- Van Schmus, W., & Ribbe, P. (1968). The composition and structural state of feldspar from chondritic meteorites. *Geochimica et Cosmochimica Acta*, *32*(12), 1327–1342. [https://doi.org/10.1016/0016-7037\(68\)90032-X](https://doi.org/10.1016/0016-7037(68)90032-X)
- Williams, Q., & Jeanloz, R. (1989). Static amorphization of anorthite at 300 K and comparison with diaplectic glass. *Nature*, *338*(6214), 413–415. <https://doi.org/10.1038/338413a0>